Effect of E20D Substitution in the Active Site of *Escherichia coli* Inorganic Pyrophosphatase on Its Quaternary Structure and Catalytic Properties†

Sergei E. Volk,‡ Valerii Yu. Dudarenkov,‡ Jarmo Käpylä,§,|| Vladimir N. Kasho,⊥ Olga A. Voloshina,‡ Tiina Salminen,||,# Adrian Goldman,# Reijo Lahti,|| Alexander A. Baykov,*,‡ and Barry S. Cooperman*,§

A. N. Belozersky Institute of Physico-Chemical Biology, Moscow State University, Moscow 119899, Russia, Department of Chemistry, University of Pennsylvania, Philadelphia, Pennsylvania 19104-6323, Center for Ulcer Research and Education, Department of Medicine, University of California, Los Angeles, California 90073, Department of Biochemistry, University of Turku, FIN-20500 Turku, Finland, and Centre for Biotechnology, 13521 Turku, Finland

Received November 6, 1995; Revised Manuscript Received February 7, 1996⊗

ABSTRACT: Glutamic acid 20 is an evolutionarily conserved residue found within the active site of the inorganic pyrophosphatase of *Escherichia coli* (E-PPase). Here we determine the effect of E20D substitution on the quaternary structure and catalytic properties of E-PPase. In contrast to wild-type enzyme, which is hexameric under a variety of conditions, E20D-PPase can be dissociated by dilution into nearly inactive trimers, as shown by electrophoresis of cross-linked enzyme, analytical ultracentrifugation, and measurement of catalytic activity as a function of enzyme concentration. Hexamer stability is increased in the presence of both substrate and Mg^{2+}, is maximal at pH 6.5, and falls off sharply as the pH is lowered or raised from this value. Measured at saturating substrate, 20 mM Mg^{2+} and pH 7.2, E20D substitution (a) decreases activity toward inorganic pyrophosphate (PP_i) hydrolysis and oxygen exchange between water and inorganic phosphate (P_i), (b) increases the rate of net PP_i synthesis, and (c) decreases the amount of enzyme-bound PP_i in equilibrium with P_i in solution. Measurements of PP_i hydrolysis rate as a function of both Mg^{2+} concentration and pH for the E20D variant show that its decreased activity is largely accounted for on the basis of an increased pK_a of the catalytically essential base at the active site, and the need for a Mg^{2+} stoichiometry of 5 in the enzyme−substrate complex, similar to what is seen for the D97E variant. By contrast, wild-type PPase catalysis over a wide range of Mg^{2+} concentration and pH is dominated by an enzyme−substrate complex having a total of four Mg^{2+} ions. These results are consistent with a supporting role for Glu20 in PPase catalysis and demonstrate that even conservative mutation at the active site can perturb the quaternary structure of the enzyme.

Soluble inorganic pyrophosphatase (EC 3.6.1.1; PPase[1]) is a ubiquitous enzyme, known to be essential for cell growth and having an active site structure and catalytic mechanism that is highly conserved evolutionarily (Cooperman et al., 1992). The simplicity of its substrate makes this enzyme an attractive model for enzyme-catalyzed phosphoryl transfer (Knowles, 1980; Herschlag & Jencks, 1990).

Escherichia coli PPase (E-PPase) is homohexameric (Wong et al., 1970), containing 175 amino acid residues per monomer (Lahti et al., 1988). The hexamer is arranged as an almost perfect octahedron formed by two trimers. Although catalysis by E-PPase is a complex function of both Mg^{2+} concentration and pH, its catalytic properties over a wide range of conditions are well accounted for by Scheme 1 (Baykov et al., 1996), where *j* is equal to 2.

The catalytic mechanism of soluble PPases involves a group of 15 conserved active site residues, identified by sequence analysis of PPases from several organisms (Cooperman et al., 1992), as well as high-resolution X-ray crystallographic structures of PPases, not only from *E. coli* (Kankare et al., 1994; Oganessyan et al., 1994) but also from *Saccharomyces cerevisiae* (Terzyan et al., 1984) and *Thermus thermophilus* (Teplyakov et al., 1994). In the past several years we have been engaged in an intensive study directed toward the elucidation of the roles of the active site residues in catalysis through characterization of the structural and functional consequences of site-specific mutagenesis of E-PPase (Lahti et al., 1990, 1991; Cooperman et al., 1992; Kankare et al., 1994, 1996a,b; Baykov et al., 1995; Käpylä et al., 1995; Salminen et al., 1995; Velichko et al., 1995).

Here we explore the consequences for both quaternary structure and catalytic function of mutating one such conserved active site residue, Glu20, to Asp and compare the functional consequences of E20D mutation with those observed on D97E mutation (Käpylä et al., 1995).

† This work was supported by grants from the NIH (DK13212 and TW00407), the International Science Foundation and Russian Government (M2J000 and M2J300), the Russian Foundation for Basic Research (94-04-12658-a), and the Finnish Academy of Sciences (Grants 1009 and 11444).

* Authors to whom to address correspondence (A.A.B.: FAX, 095-939-3181; telephone, 095-939-5541; email, abaykov@beloz.genebee.msu.su. B.S.C.: FAX, 215-898-2037; telephone, 215-898-6330; email, cooprman@pobox.upenn.edu).

‡ Moscow State University.

§ University of Pennsylvania.

|| University of Turku.

⊥ University of California.

Centre for Biotechnology.

⊗ Abstract published in *Advance ACS Abstracts,* April 1, 1996.

[1] Abbreviations: E-PPase, *Escherichia coli* inorganic pyrophosphatase; MES, 2-(*N*-morpholino)ethanesulfonic acid; P_i, inorganic phosphate; PPase, inorganic pyrophosphatase; PP_i, inorganic pyrophosphate; WT-PPase, wild-type E-PPase.

0006-2960/96/0435-4662$12.00/0

Scheme 1: Minimal Scheme of E-PPase Catalysis[a]

$$Mg_1E + Mg_2PP_i \underset{k_2}{\overset{k_1}{\rightleftharpoons}} Mg_1EMg_2PP_i \underset{k_4}{\overset{k_3}{\rightleftharpoons}} Mg_1E(MgP_i)_2 \underset{k_6}{\overset{k_5}{\rightleftharpoons}} Mg_1EMgP_i + MgP_i \underset{k_8}{\overset{k_7}{\rightleftharpoons}} Mg_1E + MgP_i$$

[a] $K_1 = k_1/k_2$; $K_3 = k_3/k_4$; $K_5 = k_5/k_6$; $K_7 = k_7/k_8$.

EXPERIMENTAL PROCEDURES

Enzyme. The expression and purification of wild type PPase (WT-PPase) and E20D-PPase from overproducing *E. coli* HB101 strain transformed with suitable plasmids derived from pUC19 were carried out as described by Lahti et al. (1990). E20D-PPase obtained in this way is contaminated with about 0.5% (by weight) endogenous, chromosomal-encoded, WT-PPase (Käpylä et al., 1995), which would have only negligible effects on most of the kinetic and binding parameters determined in this work. E20D-PPase used in the studies of hydrolysis kinetics was freed from even traces of WT-PPase by gel filtration on a Sephadex G-100 (Pharmacia) column in 0.05 M Tris−HCl (pH 7.2) at 4 °C. E20D-PPase exists in trimeric form under these conditions (Velichko et al., 1995) and is retarded on the column relative to hexameric WT-PPase. D97E-PPase was prepared free of endogenous WT-PPase contamination as described (Käpylä et al., 1995).

Stock E20D-PPase solutions, except as noted, were made in 0.1 M MES−Tris buffer (pH 6.5) containing 20 mM $MgCl_2$ and 50 μM EGTA and were preincubated for at least 1 h at 25 °C before use. Enzyme concentration was estimated on the basis of a subunit molecular mass of 20 kDa (Wong et al., 1970). Protein was determined according to Bradford (1976). Except as otherwise indicated, PPase activity was assayed in a medium containing 0.1 mM PP_i, 5 mM $MgCl_2$, 50 μM EGTA, and 0.1 M Tris-HCl (pH 9).

Kinetic and Binding Assays. Rates of PP_i hydrolysis, PP_i synthesis, and oxygen exchange between [^{18}O]P_i and H_2O were determined as described in Baykov et al. (1996), as were the amounts of enzyme-bound PP_i in equilibrium with medium P_i and Mg^{2+} and equilibrium dialysis measurements of Mg^{2+} bound to E20D-PPase. Unless otherwise indicated, Tris-HCl buffers were used to maintain pH, at concentrations maintaining the ionic strength at 0.15−0.20 M. EGTA (50 μM) was included in all solutions containing enzyme. All experiments reported were carried out at 25 °C.

Cross-Linking and Electrophoresis. Cross-linking of PPases with glutaraldehyde and subsequent SDS−PAGE analysis were carried out as described in Baykov et al. (1995). Protein bands were visualized with Coomassie Blue R-250. The standard proteins were carbonic anhydrase (30 kDa), egg albumin (43 kDa), bovine serum albumin (67 kDa), and phosphorylase *b* (94 kDa).

Sedimentation. Sedimentation velocity measurements were carried out at as described in Baykov et al. (1995). The solutions contained 10 mM enzyme, varying $MgCl_2$ concentration, 50 μM EGTA, 0.5 mM dithiothreitol, and either 0.1 M MES−Tris (pH 6.5) or 0.05 M Tris−HCl (pH 7.2 or 8.5).

RESULTS

Dissociation of E20D-PPase into Trimers. Previous studies indicated that E20D substitution in E-PPase increased Nile Red binding (at pH 8.0 in the absence of Mg^{2+}), electrophoretic mobility (Salminen et al., 1995) and cold lability (Velichko et al., 1995), and that the latter effect was due to a dissociation of hexameric PPase into trimers, as shown by sedimentation velocity analysis. Evidence for the formation of trimers at 25 °C comes from SDS−PAGE analysis of both E20D-PPase and WT-PPase subjected to glutaraldehyde treatment at pH 8.5 in the absence of Mg^{2+}. As seen in Figure 1, the predominant form of the cross-linked E20D-PPase is trimeric and no band corresponding to hexameric protein is observed. In contrast, cross-linking of WT-PPase yields bands corresponding to both trimeric and hexameric forms. The sedimentation results presented in Table 1 demonstrate that trimers formed by E20D-PPase at 25 °C are characterized by a sedimentation coefficient of 3.3 and that trimer formation is favored by low Mg^{2+} concentration and high pH. By contrast, WT-PPase is predominantly hexameric (sedimentation coefficient 5.9−6.2) under all conditions tested, in accord with the data of Wong et al. (1970).

Table 1: Sedimentation Coefficients[a]

pH	[$MgCl_2$] (mM)	$s_{20,w}$ E20D-PPase	$s_{20,w}$ WT-PPase
6.5	20	5.9 ± 0.1	
7.2	1	~6[b]	6.2 ± 0.2
8.5	1	3.3 ± 0.2	5.9 ± 0.2
8.5	20	6.0 ± 0.2	6.1 ± 0.3

[a] Measured at 10 μM protein concentration. [b] Apparent heterogeneity; the value given refers to the major component.

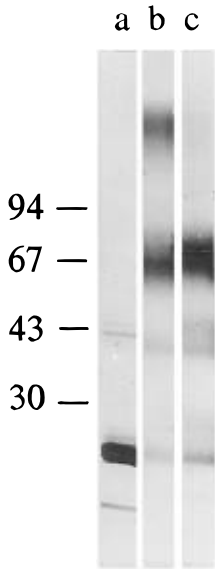

FIGURE 1: SDS−PAGE analysis of WT-PPase and E20D-PPase: (a) intact E20D-PPase; (b) cross-linked WT-PPase; (c) cross-linked E20D-PPase.

The E20D-PPase Trimer Has Low Specific Activity. The specific activity of E20D-PPase depends markedly on enzyme concentration (Figure 2). By contrast, the specific activity of WT-PPase at pH 7.2 is constant over the concentration range 0.1−50 μM. The results for E20D-PPase can be accounted for quantitatively by eqs 1a−c,

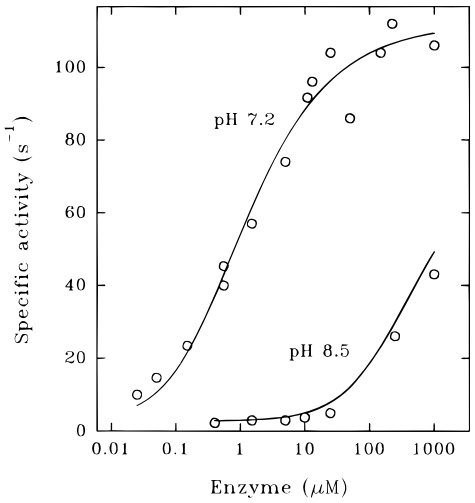

FIGURE 2: Specific activity of E20D-PPase preequilibrated at different enzyme concentrations at pH 7.2 or 8.5. Preincubations were for 5 h at pH 7.2 or 0.5 − 2 h at pH 8.5 in the presence of 0.05 M Tris-HCl and 1 mM $MgCl_2$. The lines are drawn according to eqs 2a−c, using the best-fit parameters shown in Table 2.

Scheme 2[a]

$$H \underset{k_a}{\overset{k_d}{\rightleftharpoons}} 2T$$

[a] $K_d = k_d/k_a$.

Table 2: Rate and Equilibrium Constants for Scheme 2[a]

pH	k_d (h^{-1})[b]	k_a (mM^{-1} h^{-1})	K_d (μM)	A_H (s^{-1})	A_T (s^{-1})
6.5	0.30 ± 0.05				
7.2	0.85 ± 0.14	1.7 ± 0.8	0.46 ± 0.15	112 ± 3	5.6 ± 3.7
8.5	420 ± 30	1.6 ± 0.4	262 ± 46	78 ± 15	2.0 ± 0.4

[a] Measured at 1 mM Mg^{2+}. [b] Measured following a 220-fold dilution of 11 μM enzyme which had been preequilibrated at pH 7.2 in the presence of 1 mM Mg^{2+}.

which are derived from the hexamer−trimer equilibrium depicted in Scheme 2 (Kurganov, 1982). Here, k_d and k_a are dissociation and association rate constants, the hexamer H and trimer T have specific activities of A_H and A_T, respectively, $\alpha_{H,eq}$ is the fraction of enzyme in the hexameric

$$A = A_T + (A_H - A_T)\alpha_{H,eq} \quad (1a)$$

$$\alpha_{H,eq} = 6[H]/[E]_t = (z - 1)/(z + 1) \quad (1b)$$

$$z = (1 + 8[E]_t/3K_d)^{1/2} \quad (1c)$$

form at equilibrium, and $[E]_t$ is total enzyme concentration, expressed in monomers. Values of A_H, A_T, and K_d at pH 7.2 and 8.5 were estimated by nonlinear regression analysis of the data shown in Figure 2. K_d was found to increase from 0.46 μM at pH 7.2 to 262 μM at pH 8.5 (Table 2). At both pH values, as well as at pH 9.0 (data not shown), $A_T \leq 0.05A_H$.

Two additional observations are consistent with the notion that E20D-PPase inactivation on dilution is caused by reversible enzyme dissociation. First, the effects of pH and Mg^{2+} concentration on activity (Figures 2 and 3) parallel their effects on the sedimentation coefficient (Table 1). On the basis of Figure 2, the fraction of the hexameric form is about 80% at pH 7.2 and only 1% at pH 8.5 at 10 μM protein concentration, in agreement with the sedimentation results.

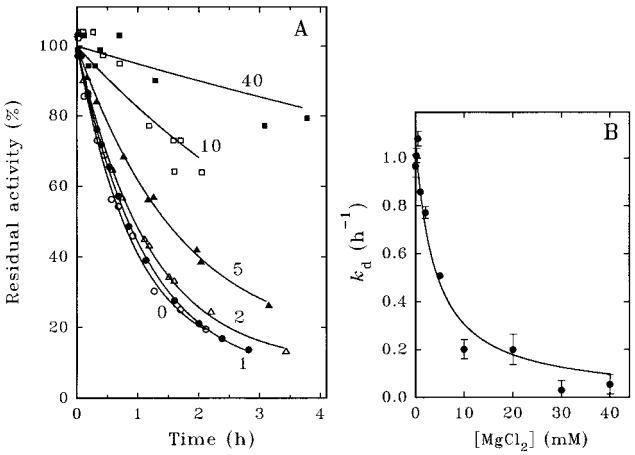

FIGURE 3: Protection of E20D-PPase by Mg^{2+} against inactivation on dilution. (A) Time courses of the inactivation in the presence of 0 (○), 1 (●), 2 (△), 5 (▲), 10 (□), and 40 (■) mM $MgCl_2$. Stock enzyme solution (25 mM, pH 6.5) was diluted 500-fold into a solution containing 0.22 M Tris-HCl, pH 7.2, 50 mM dithiothreitol, 50 μM EGTA, and varied levels of $MgCl_2$, incubated for indicated time intervals at 25 °C and assayed for residual activity. The curves represent the best fit for eq 3. (B) Dissociation rate constant, as calculated from (A), against Mg^{2+} concentration. The line is drawn to eq 4, using K_M = 4.0 mM and $k_{d,lim}$ = 0.108 h^{-1}.

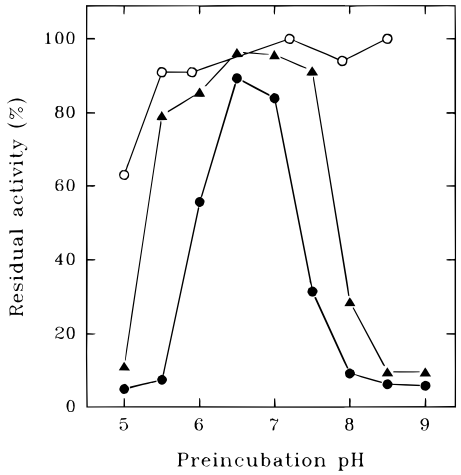

FIGURE 4: Effect of preincubation at different pH values on the activity of WT (○) and E20D-PPase (▲, ●). Stock enzyme solutions (50 mM, pH 6.5) were diluted 200-fold into solutions of varying pH as indicated on the abscissa, incubated for 15 s (▲) or 20 min (○, ●) and assayed for residual activity. The activity measured without any preincubation in the absence of substrate (110 s^{-1} for E20D-PPase and 205 s^{-1} for WT-PPase) was taken as 100% in each case. The buffers used were 0.1 M MES−Tris (pH 5−6.5) or Tris-HCl (pH 7−9) and contained 1 mM $MgCl_2$ and 50 μM EGTA.

Second, shifting a 25 μM solution of E20D-PPase from pH 8.5, 1 mM Mg^{2+}, where it has only low specific activity (5% of hexamer), to pH 7.2, 1 mM Mg^{2+}, results in an activation to 80% of the hexamer activity, as predicted from the values derived for K_d, A_H, and A_T.

Stabilization of Hexameric E20D-PPase. The results presented in Figure 3 and Table 1 clearly demonstrate the stabilization of the hexameric enzyme by relatively high concentrations of Mg^{2+}. At low (1 mM) [Mg^{2+}] enzyme activity, and hence hexamer stability, is maximal at pH 6.5, and falls off sharply as the pH is lowered or raised from this value (Figure 4). First-order rate constants for E20D-PPase inactivation (dissociation) at three pH values (Table 2), estimated from time courses of activity following enzyme dilution using eq 2 (Kurganov, 1982), lead to the conclusion

Table 3: Rates of PP_i Synthesis Catalyzed by E20D-PPase and D97E-PPase[a]

variant	$[MgP_i]$ (mM)	v_s (s^{-1})	k_s (s^{-1})
E20D	21	3.4	5.3
E20D	28	4.6	6.5
E20D	35	5.3	7.1
D97E	20	0.132	0.174

[a] Measured at pH 7.2 and 20 mM Mg^{2+}.

Table 4: Kinetic Parameters for P_i-H_2O Oxygen Exchange Catalyzed by E20D-PPase[a]

total Mg^{2+} (mM)	free Mg^{2+} (mM)	P_c	v_{ex} (s^{-1})
2	0.63	0.076	0.092
5	1.7	0.076	0.66
10	3.8	0.065	2.3
20	9.5	0.067	3.3
30	16.7	0.061	6.2
34	20	0.078	6.3
50	34	0.069	6.8

[a] Measured at pH 7.2 and 20 mM total P_i concentration.

that pH effects on K_d parallel those on k_d.

$$\alpha_H = (\alpha_{H,eq} + e^{-zk_dt})/(1 + \alpha_{H,eq}e^{-zk_dt}) \quad (2)$$

Substrate PP_i, or its Mg^{2+} complexes, also stabilizes the hexamer. Thus, although incubation of enzyme at pH 8.5 with 1 mM Mg^{2+} prior to PP_i addition results in rapid inactivation ($t_{1/2} \sim 10$ s), addition of 0.1 mM PP_i at various times during such incubation leads to strictly linear Pi formation for at least 3 min, i.e., no further inactivation occurs following PP_i addition.

Analysis of the protection afforded by Mg^{2+} against enzyme dissociation (Figure 3) according to eq 3, where $k_{d,lim}$ is the value of k_d at saturating $[Mg^{2+}]$, affords an estimate of a dissociation constant for Mg^{2+} binding, K_M, of 4 ± 2 mM.

$$k_d = k_{d,lim}/(1 + [Mg^{2+}]/K_M) \quad (3)$$

Hexameric E20D-PPase Catalysis of PP_i-P_i Equilibration. Rate and Equilibrium Constants at pH 7.2 and 20 mM Mg^{2+}. Earlier we evaluated all rate and binding constants shown in Scheme 1 for WT-PPase, as well as some for D97E-PPase (Baykov et al., 1990, 1996; Käpylä et al., 1995). In addition to steady-state rates of PP_i hydrolysis (v_h), these involved measurements of steady-state rates of PP_i synthesis (v_s) and P_i-H_2O oxygen exchange (v_{ex}), as well as of equilibrium enzyme-bound PP_i (EPP_i) formation, as a function of $[MgP_i]$. Here we use the same approach to evaluate the same constants for hexameric E20D-PPase and extend the measurement of v_s to D97E-PPase. The experiments are carried out at 20 mM Mg^{2+} and pH 7.2 for direct comparison with results obtained earlier with WT-PPase and D97E-PPase.

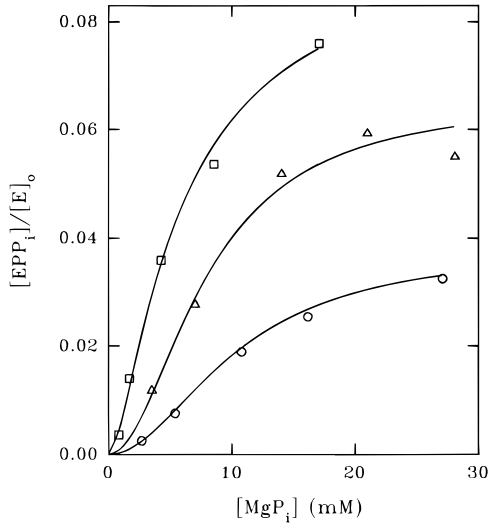

FIGURE 5: Formation of enzyme-bound PP_i by E20D-PPase at pH 7.2. The free Mg^{2+} concentration was fixed at 10 (○), 20 (△), or 50 (□) mM. Lines are drawn to eq 5. The points shown are the average of two to five measurements.

Values for K_3, K_5, and K_7 were determined by fitting the observed dependence of EPP_i formation to eq 4, in which $[E]_t$ refers to the total enzyme concentration in solution and [EPPi] refers to the total concentration of all forms of enzyme-bound PP_i (Figure 5).

$$[EPP_i]/[E]_t = 1/(K_3K_5K_7/[MgP_i]^2 + K_3K_5/[MgP_i] + K_3 + 1) \quad (4)$$

Values of the catalytic constants for PP_i synthesis (k_s) and

Table 5: Rate and Equilibrium Constants for PPase Catalysis[a]

parameter	WT-PPase[b]	E20D-PPase[c]	D97E-PPase[b]
K_m (μM)	3.5 ± 0.5, 2.1 ± 0.2[d]	1.6 ± 0.1	1.8 ± 0.2
k_h (s^{-1})	155 ± 8	38 ± 2	12 ± 1
k_s (s^{-1})	2.0 ± 0.5[d]	6.3 ± 0.5	0.174 ± 0.015[e]
k_{ex} (s^{-1})	116 ± 21	11.6 ± 1.5	0.34 ± 0.03
P_c	0.24 ± 0.03	0.068 ± 0.007	<0.01
K_1 (μM^{-1})	2.3 ± 0.6	0.31 ± 0.20	0.19 ± 0.08, 0.67 ± 0.29[e]
K_3	5.8 ± 0.6	12 ± 2	56 ± 6
K_5 (mM)	7.4 ± 1.2	8 ± 5	5.7 ± 1.6
K_7 (mM)	1.6 ± 0.2	3 ± 2	2.5 ± 0.7
k_1 (μM^{-1} s^{-1})	46 ± 5	49 ± 14	14 ± 5[e]
k_2 (s^{-1})	20 ± 5	160 ± 70	21 ± 5[e]
k_3 (s^{-1})	800 ± 180	150 ± 40	19 ± 2
k_4 (s^{-1})	140 ± 30	13 ± 2	0.34 ± 0.09
k_5 (s^{-1})	440 ± 110	180 ± 40	>45
k_6 (mM^{-1} s^{-1})	59 ± 17	22 ± 18	
k_7 (s^{-1})	400 ± 100	74 ± 26	>45
k_8 (mM^{-1} s^{-1})	260 ± 70	27 ± 50	

[a] Measured at pH 7.2 and 20 mM Mg^{2+}. [b] Measured by Käpylä et al. (1995), except as noted. [c] Hexameric form. [d] Measured by Baykov et al. (1990). [e] This work. k_2 was calculated from eq 10. k_1 is equal to $(1 + k_2/k_3 + k_2k_4/k_3k_5)k_h/K_m$ (Baykov et al., 1996). K_1 is equal to k_1/k_2.

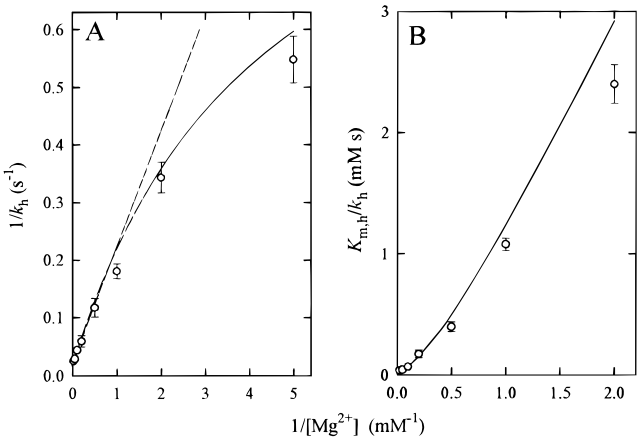

FIGURE 6: Michaelis−Menten parameters for PP_i hydrolysis by E20D-PPase at pH 7.2 as functions of free Mg^{2+} concentration. (A) $1/k_h$ vs $1/[Mg^{2+}]$. The solid line is drawn to eq 5, using parameter values in Table 6. The dashed line is a best fit straight line through data taken at $[Mg^{2+}] \geq 0.02$ mM. (B) $K_{m,h}/k_h$ vs $1/[Mg^{2+}]$. The line is drawn to eq 6, using the parameter values in Table 6.

oxygen exchange (k_{ex}) were obtained by extrapolating measured v_s (Table 3) and v_{ex} (Table 4) to saturating $[MgP_i]$, as described by Käpylä et al. (1995). The partition coefficient, P_c (Table 4), which measures the probability of PP_i formation from enzyme-bound P_i vs P_i dissociation [$k_4/(k_4+k_5)$], was calculated from the distributions of five ^{18}O-labeled P species during the P_i-H_2O oxygen exchange (Hackney & Boyer, 1978; Hackney, 1980; Springs et al., 1981).

The rate and equilibrium constants estimated or derived from these measurements are collected and compared with those determined for WT-PPase in Table 5, from which it is clear that, measured at saturating substrate, 20 mM Mg^{2+} and pH 7.2, E20D substitution (a) decreases hydrolytic activity (k_h) and oxygen-exchange activity (k_{ex}), (b) increases synthetic activity (k_s), (c) destabilizes the EPP_i complex (K_3), and (d) increases k_2 and decreases k_3-k_8, while leaving k_1 unchanged.

In the sections that follow, these measurements are extended by determination of the dependencies of k_h and k_h/K_m on Mg^{2+} concentration at fixed pH (7.2) and on pH at fixed Mg^{2+} concentration (20 mM), in order to more fully elucidate the underlying reason(s) for the latter observations.

Hexameric E20D-PPase Catalysis of PP_i Hydrolysis. Dependence on Mg^{2+} Concentration. For WT-PPase at pH 7.2, both k_h and k_h/K_m as a function of Mg^{2+} concentration are well saturated by 20 mM (Käpylä et al., 1995). Such is not the case for E20D-PPase (Figure 6), for which 20 mM Mg^{2+} is inadequate to achieve saturation. WT-PPase binds two Mg^{2+} per subunit with relatively high affinity in the absence of substrate (Käpylä et al., 1995; Volk et al., 1996). The results of equilibrium dialysis experiments, conducted at enzyme concentrations (≥0.5 mM) high enough that hexamer is the dominant form even in the absence of Mg^{2+}, indicate that E20D substitution is virtually without effect on the binding of the first Mg^{2+} (K_{m1}) and only weakens the binding of the second Mg^{2+} (K_{m2}) by a factor of 3 (Table 6). This small effect is inadequate to account for the observed dependence of k_h and k_h/K_m on Mg^{2+} concentration.

Scheme 3A describes a minimal model providing an acceptable fit, based on low values of mean relative deviation of calculated vs measured values compared to experimental error and the absence of systematic deviation, to measurements of the velocity of PP_i hydrolysis as a function of the concentrations of Mg^{2+} and Mg_2PP_i at pH 7.2 (Figure 6). In this model conversion of substrate to product proceeds via two enzyme substrate complexes, having total Mg^{2+} stoichiometries of 4 (M_2ES) or 5 (M_3ES), in accord with the curvature of the plot in Figure 6A. Fitting the data in Figure 6 to eqs 5 and 6, derived from Scheme 3A, yielded the parameter values displayed in Table 6. These parameters make clear that (a) at low $[Mg^{2+}]$ (0.2 mM) binding of substrate proceeds mainly via M_2E and hydrolysis proceeds via both M_2ES_t and M_3ES_t; (b) at $[Mg^{2+}]$ of 1 mM, substrate binding proceeds via both M_2E_t and M_3E_t but the dominant hydrolysis pathway is via M_3ES_t; (c) at $[Mg^{2+}] \geq 5$ mM the dominant substrate binding pathway is via M_3E_t and the dominant hydrolysis pathway is via M_3ES_t; and (d) dissociation of the enzyme−substrate complex proceeds mainly or exclusively via M_3ES_t over a wide range of Mg^{2+} concentration.

Table 6: Equilibrium and Rate Constants for Scheme 3[a]

	WT-PPase[b]	E20D-PPase[c]	D97E-PPase[d]
K_{m1} (mM)[e]	0.080 ± 0.003	0.12 ± 0.02	0.076 ± 0.02
K_{m2} (mM)[e]	1.7 ± 0.2	6 ± 2	1.9 ± 0.1
K_{m3} (mM)	25 ± 6	21 ± 5	61 ± 40
$k_1^{(2)}$ (μM^{-1} s^{-1})	167 ± 16	21 ± 6	2 ± 0.6
$k_1^{(3)}$ (μM^{-1} s^{-1})	nd[f]	320 ± 60	80 ± 40
$k_2^{(2)}$ (s^{-1})	12	<5	1.4 ± 0.8
$k_2^{(3)}$ (s^{-1})	<2	280 ± 140	27 ± 13
$K_{a3,app}$ (mM)	>50	15 ± 2	6.3 ± 0.9
K^{H2}_{a3} (mM)	undetected	12 ± 3	17 ± 6
K^{H}_{a3} (mM)	>50	<10[g]	<30[g]
$K^{H}_{a3}k_h^{(2)}$ (mM s^{-1})	>10000	20 ± 9	100 ± 30
$k_{h,app}^{(2)}$ (s^{-1})	139	0.9 ± 0.3	0.9 ± 0.2
$k_h^{(2)}$ (s^{-1})	199 ± 8	>2.5[g]	>4[g]
$k_{h,app}^{(3)}$ (s^{-1})	undetected	59 ± 4	14.7 ± 0.5
$k_h^{(3)}$ (s^{-1})	undetected	126 ± 10	120 ± 10
pK'_{ESH2}	<6	7.50 ± 0.08 (7.7 ± 0.1)[h]	7.90 ± 0.09 (8.1 ± 0.1)[h]
pK_{ESH2}	6.7 ± 0.7	>7.5	>7.9
pK'_{ESH}	<9.2	(10.2 ± 0.1)[i]	(9.9 ± 0.1)[i]
pK_{ESH}	10.04		

[a] Derived from initial velocity experiments except as indicated. [b] Derived from values in Baykov et al. (1990, 1995, 1996). [c] This work. Initial parameter values for data at pH 7.2 and varying Mg^{2+} concentration were obtained as follows. k_h values were first fit to eq 5, providing values for $K_{a3,app}$, $k_{h,app}^{(2)}$, and $k_{h,app}^{(3)}$. The remaining parameters were obtained from eq 6, and the value determined for k_2 at 20 mM Mg^{2+} (Table 5), using the relationship $k_2 = (k_2^{(2)} + k_2^{(3)}[Mg^{2+}]/K_{a3,app})/(1 + [Mg^{2+}]/K_{a3,app})$. Final parameter values were obtained by simultaneous fitting of all velocity measurements (108 points) to eq 6. pH-independent parameters were derived using data taken in the pH range 6.0−9.0. [d] Derived from values in Käpylä et al. (1995) and in Table 5. [e] From dialysis experiments. Experimental conditions for measurements with the E20D variant: 0.51−0.76 mM enzyme and 0.03−1.8 mM Mg^{2+}. [f] Not determined. [g] See Discussion. [h] Apparent pK_a for loss of a proton from a mixture of H_2Mg_3ES and H_2Mg_2ES at 20 mM Mg^{2+}. [i] Apparent pK_a for loss of a proton from a mixture of HMg_3ES and HMg_2ES at 20 mM Mg^{2+}.

$$k_h = \frac{k_{h,app}^{(3)} + k_{h,app}^{(2)} K_{a3,app}/[Mg^{2+}]}{1 + K_{a3,app}/[Mg^{2+}]} \quad (5)$$

$$k_h/K_m = FG/QR \quad (6)$$

where $F = k_1^{(2)} + k_1^{(3)}[Mg^{2+}]/K_{m3}$; $G = k_{h,app}^{(2)} + k_{h,app}^{(3)}[Mg^{2+}]/K_{m3}$; $Q = 1 + K_{m1}K_{m2}/[Mg^{2+}]^2 + K_{m2}/[Mg^{2+}] + [Mg^{2+}]/K_{m3}$; and $R = k_2^{(2)} + k_2^{(3)}[Mg^{2+}]/K_{a3,app} + k_{h,app}^{(2)} + k_{h,app}^{(3)}[Mg^{2+}]/K_{a3,app}$.

Scheme 3: PP_i Hydrolysis as a Function of Mg^{2+} Concentration and pH[a]

(A) Dependence of k_h and k_h/K_m on Mg^{2+} Concentration at pH 7.2

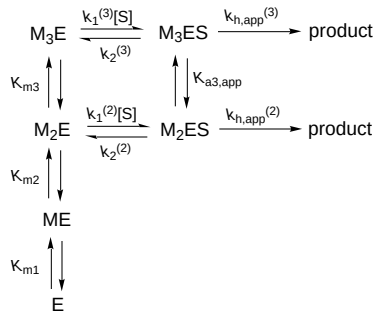

(B) Dependence of k_h on pH and Mg^{2+}

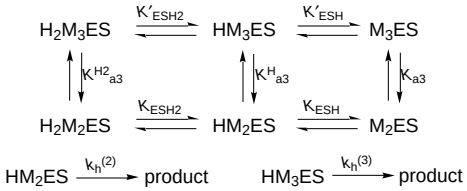

[a] Definitions: $K_{m1} = [Mg^{2+}][E]_t/[ME]_t$; $K_{m2} = [Mg^{2+}][ME]_t/[M_2E]_t$; $K_{m3} = [Mg^{2+}][M_2E]_t/[M_3E]_t$. $K_{a3,app} = [Mg^{2+}][M_2ES]_t/[M_3ES]_t$; $K_{a3} = [Mg^{2+}][M_2ES]/[M_3ES]$. $K^{H}_{a3} = [Mg^{2+}][HM_2ES]/[HM_3ES]$; $K^{H2}_{a3} = [Mg^{2+}][H_2M_2ES]/[H_2M_3ES]$. $K'_{ESH2} = [H^+][HM_3ES]/[H_2M_3ES]$; $K'_{ESH} = [H^+][M_3ES]/[HM_3ES]$. $K_{ESH2} = [H^+][HM_2ES]/[H_2M_2ES]$; $K_{ESH} = [H^+][M_2ES]/[HM_2ES]$. S is Mg_2PP_i. The letter t refers to all protonated forms of E, M_jE, and M_jES.

Table 7: k_h and k_h/K_m Values for E20D-PPase: pH Dependence[a]

pH[b]	k_h (s^{-1})	k_h/K_m (μM^{-1} s^{-1})
6.5	6.4 ± 0.1 (7.3)	3.6 ± 0.2
7.2	38 ± 2 (30)	26 ± 3
7.9	71 ± 3 (76)	36 ± 3
8.5	105 ± 4 (109)	32 ± 2
9.0	124 ± 4 (120)	37 ± 2
9.8	91 ± 10	25 ± 4
10.4	53 ± 4	7.2 ± 0.5

[a] At 20 mM Mg^{2+}. Values in parentheses are calculated from eq 7, using parameter values in Table 6. [b] Buffers employed: pH 6.5, 0.05 M MES−Tris; pH 7.2, 0.15 M Tris-HCl; pH 7.9−9.0, 0.1 M 2-amino-2-methyl-1,3-propanediol−HCl; pH 9.8 and 10.4, 0.15 M 3-(cyclohexylamino)-1-propanesulfonic acid−KOH.

Hexameric E20D-PPase Catalysis of PP_i Hydrolysis. Dependence on pH. k_h and k_h/K_m were determined as a function of pH at 20 mM Mg^{2+} (Table 7), allowing calculation of pH-independent values for k_h/K_m of 44 ± 9 μM^{-1} s^{-1} and for k_h of 130 ± 14 s^{-1}. The clear pH optimum for k_h indicates that for E20D-PPase, as for WT-PPase (Baykov et al., 1996), conversion of substrate to product depends on both an essential base and an essential acid.

Scheme 3B describes a minimal model providing an acceptable fit to k_h values measured as a function of both Mg^{2+} concentration (at pH 7.2) and pH (6.0−9.0 at 20 mM Mg^{2+}). Fitting k_h values to eq 7, derivable from Scheme 3B, permitted evaluation of several of the parameters in this equation, as displayed in Table 6. For the values fitted, the term $K'_{ESH}/[H^+](1 + K_{a3}/[Mg^{2+}])$ was negligible and could be omitted, so no estimation of K'_{ESH} or K_{a3} was attempted. From the values obtained it is clear, comparing the values of $k_h^{(3)}$ and $k_h^{(2)}K^{H}_{a3}/[Mg^{2+}]$, that over the entire pH range, and at $[Mg^{2+}] > 0.5$ mM, hydrolysis proceeds essentially exclusively via the HMg_3ES complex.

$$k_h = (k_h^{(3)} + k_h^{(2)}K^{H}_{a3}/[Mg^{2+}])/(1 + K^{H}_{a3}/[Mg^{2+}] + [H^+]/K'_{ESH2}(1 + K^{H2}_{a3}/[Mg^{2+}]) + K'_{ESH}/[H^+](1 + K_{a3}/[Mg^{2+}])) \quad (7)$$

It only proved possible to evaluate the product $k_h^{(2)}K^{H}_{a3}$, and not the individual constants making up this term, so that only limiting values could be estimated for $k_h^{(2)}$ and K^{H}_{a3}. The lower limit value for $k_h^{(2)}$ of >2.5 s^{-1} (and consequently the upper limit value of K^{H}_{a3} of <8.5 mM) is based on the value of $k_{h,app}^{(2)}$ at pH 7.2 and the assumption that $pK_{ESH2} \geq pK'_{ESH2}$. This assumption is consistent with the results obtained for WT-PPase ($pK_{ESH2} \geq pK'_{ESH2}$; $pK_{ESH} \geq pK'_{ESH}$; Table 6) and is in accord with the expectation, based on simple electrostatics, that binding of an additional Mg^{2+} should, if anything, lower rather than raise the pK_a of a given group. More precise estimation of $k_h^{(2)}$ and K^{H}_{a3} would require that k_h values be obtained as a function of varying Mg^{2+} at higher pH. Unfortunately, the tendency of PPase to dissociate into trimers at high pH and low Mg^{2+} concentration limited our ability to perform such experiments.

DISCUSSION

Effect of E20D Substitution on Subunit Interaction. Although Glu 20 is located within the active site cavity, at a distance of some 15 Å from the nearest portion of the trimer−trimer interface in E-PPase (Kankare et al., 1996a,b), its substitution by an Asp markedly weakens E-PPase quaternary structure, with the result that E20D-PPase can be dissociated into trimers as a function of pH and enzyme concentrations, as found in this work, or temperature, as reported previously (Velichko et al., 1995). This linkage of quaternary structure and active site is also shown by the stabilization of hexamer on binding of the active site ligands, Mg_2PP and Mg^{2+}. The similarity of the value for K_M (4 ± 2 mM; eq 3) and K_{m2} (6 ± 2 mM; Table 6) suggests that it is Mg^{2+} binding to the second of three sites we have identified on E-PPase (Baykov et al., 1996) that accounts for this stabilization. Structurally, the linkage derives from the involvement of Glu 20 both in the active site and, via its free carboxylate group, in a hydrogen bond to the backbone nitrogen of Ile 32 that stabilizes a loop structure forming part of the trimer−trimer interface (Kankare et al., 1996a). We believe it probable that, in the E20D variant, the 20−32 hydrogen bond forms poorly or not at all, allowing the loop greater mobility and weakening trimer−trimer interaction.

The value of K_d for E20D-PPase increases by $10^{2.8}$-fold between pH 7.2 and pH 8.5 (Table 2). This is consistent with our recent identification of two His residues, His 136 and His 140, at the subunit interface and the evidence that the protonation state of the subunit favoring association is one in which two His residues share a single acidic proton (Baykov et al., 1995; Kankare et al., 1996b). Linkage of quaternary and active site effects emphasizes the importance of direct structural information for the interpretation of the functional effects of amino acid substitution in proteins, as has been previously shown for ribulose-1,5-bisphosphate carboxylase (Soderling et al., 1992) and phosphoglycerate mutase (White et al., 1993).

The low catalytic activity of trimeric *E. coli* E20D-PPase toward PP_i hydrolysis is one example of an apparent general phenomenom that hexamer formation improves the catalytic

characteristics of PPase, even though each active site in E-PPase is formed by residues coming from only one subunit (Kankare et al., 1994). Thus, the trimers of E-PPase and its H136Q and H140Q variants, while retaining high k_h values, have drastically increased $K_{m,h}$ values (Baykov et al., 1995), and the trimeric forms of structurally related PPases of *Bacillus stearothermophilus* and thermophilic bacterium PS-3, obtained by simple dilution of enzyme, are both inactive (Hachimori et al., 1979; Schreier, 1980). These results, too, may be explicable on the basis of the design of the enzyme (Kankare et al,, 1996b).

Effect of E20D Substitution on Catalytic Efficiency. The dependence of E-PPase catalytic effciency on both pH and Mg^{2+} concentration presents a significant challenge for our efforts to understand the effects of the E20D mutation at the level of changes in truly microscopic rate or equilibrium constants. The strategy we have pursued in this paper is to first conduct a series of experiments at fixed pH (7.2) and Mg^{2+} concentration (20 mM), permitting effects on the rate parameters measuring catalytic efficiency, k_h, k_h/K_m, k_s, and k_{ex}, to be explained in terms of changes in the apparent (i.e., pH and Mg^{2+} concentration dependent) microscopic constants k_1-k_8 and to then explore the pH and Mg^{2+} concentration dependence of the two parameters, k_h and k_h/K_m, that are both most relevant physiologically and easiest to measure.

Measured at pH 7.2 and 20 mM Mg^{2+} E20D substitution results in large (5−10-fold) decreases in k_h and k_{ex}, as well as a 3-fold increase in k_s (Table 5). Equations 8−10 express the values of the measured rate parameters in terms of k_2-k_5, k_7, and K_3.

$$k_h = k_3k_5k_7/[k_3k_5 + k_7(k_3 + k_4 + k_5)] \quad (8)$$

$$k_{ex} = k_3k_5/[(k_5 + 0.25k_4)(K_3 + 1)] \quad (9)$$

$$k_s = k_2k_4/[k_2 + k_4(K_3 + 1)] \quad (10)$$

The large decreases in k_h and k_{ex} for E20D-PPase relative to WT-PPase are explainable in terms of decreases in k_3, k_4, k_5, and k_7. By contrast, the large decreases in k_h and k_{ex} following D97E substitution derive almost exclusively from large reductions in k_3 and k_4, respectively; i.e., $k_h \sim k_3$; $k_{ex} \sim k_4$.

The increase in the value of k_s for E20D-PPase is directly traceable to a large increase in k_2 that overcomes the much smaller increase in K_3 as well as the decrease in k_4. This large increase is correlated with a change in the dominant mode of substrate release, which is from M_3ES_t (rate constant $k_2^{(3)}$) for E20D-PPase and from M_2ES_t (rate constant $k_2^{(2)}$) for WT-PPase (Table 6). Thus the presence of a total of five Mg^{2+} ions per subunit in E20D-PPase appears to have the effect of substantially reducing the energy barrier toward substrate release. The dominant mode of substrate release is from M_3ES_t for D97E-PPase as well. However, again in contrast with E20D substitution, D97E substitution decreases the value of k_s relative to that obtained for WT-PPase, in this case because of the low value of k_4.

E20D-PPase catalysis of PP_i hydrolysis requires both a general acid and a general base, a property it shares with WT-PPase (Käpylä et al., 1995; Baykov et al., 1996). For WT-PPase hydrolysis proceeds mostly via the HMg_2ES complex. The reactivity of the HMg_3ES complex could not, however, be determined, since the combination of a high K^H_{a3} value and a relatively low pK'_{ESH} makes this species relatively inaccessible. In contrast, for the E20D variant, hydrolysis proceeds mainly via the HMg_3ES complex (Table 6).

The parameter values displayed in Table 6 provide clear explanations for the lower values of both $k_{h,app}^{(2)}$ and k_h for E20D-PPase compared with WT-PPase. From Scheme 3B, when, as is the case for E20D-PPase, the product $k_h^{(2)}K^H_{a3}$ as well as K^{H2}_{a3} and K'_{ESH2} are well determined, a higher value of $k_h^{(2)}$ requires a higher value of pK_{ESH2}. For example, if $k_h^{(2)}$ were equal to $k_h^{(3)}$ (126 s^{-1}), pK_{ESH2} would be 9.4, whereas if $k_h^{(2)}$ were equal to its lower limit of 2.5 s^{-1}, pK_{ESH2} would be 7.6. Thus, the much lower value of $k_{h,app}^{(2)}$ for E20D-PPase than for WT-PPase is due to a higher pK_a for removal of the proton from the essential base (pK_{ESH2} for WT-PPase is 6.7) and perhaps to a lower value of $k_h^{(2)}$ as well. Measured at 20 mM Mg^{2+}, the relevant pK_a for deprotonation of the essential base is pK'_{ESH2} (7.5). Thus, the lower value of k_h measured at 20 mM Mg^{2+} and pH 7.2 (Table 5) is mostly due to the only limited deprotonation of the essential base, with additional contributions from a lack of saturation of the enzyme with Mg^{2+} as well as a slightly lower value of k_h for the most reactive species (199 s^{-1} for WT-PPase vs 126 s^{-1} for E20D-PPase).

Earlier we showed that D97E-PPase shares with E20D-PPase the properties of a requirement for five Mg^{2+} in the hydrolytically active complex and a higher pK_a than WT-PPase for removal of the proton from the essential base (Käpylä et al., 1995). Scheme 3B, which clearly demonstrates the linkage between these two phenomena, well accounts for the data obtained with D97E-PPase, affording the rate and equilibrium parameter values displayed in Table 6. The general similarity of these values to those obtained with E20D-PPase demonstrates that conservative mutation of the two active site residues, Glu 20 and Asp 97, has similar consequences for these parameters. We already have demonstrated that, as measured at 20 mM Mg^{2+}, conservative mutation of a large number of active site mutants raises the pK_a for proton removal from the essential base (Salminen et al., 1995). It remains to be seen whether this effect is generally linked to a requirement for a Mg^{2+} stoichiometry of five in the active complex.

ACKNOWLEDGMENT

We thank Drs. S. Rodin, P. V. Kalmykov, and N. N. Magretova for their help in this work.

REFERENCES

Baykov, A. A., & Shestakov, A. S. (1992) *Eur. J. Biochem. 206*, 463−470.

Baykov, A. A., Shestakov, A. S., Kasho, V. N., Vener, A. V., & Ivanov, A. H. (1990) *Eur. J. Biochem. 194*, 879−887.

Baykov, A. A., Dudarenkov, V. Yu., Käpylä, J., Salminen, T., Hyytia, T., Kasho, V. N., Husgafvel, S., Cooperman, B. S., Goldman, A., & Lahti, R. (1995) *J. Biol. Chem. 270*, 30804−30812.

Baykov, A. A., Hyytia, T., Volk, S. E., Kasho, V. N., Vener, A. V., Goldman, A., Lahti, R., & Cooperman, B. S. (1996) *Biochemistry, 35*, 4655−4661.

Bradford, M. M. (1976) *Anal. Biochem. 72*, 248−254.

Cooperman, B. S., Baykov, A. A., & Lahti, R. (1992) *Trends Biochem. Sci. 17*, 262−266.

Hachimori, A., Shiroya, Y., Hirato, A., Miyahara, T., & Samejima, T. (1979) *J. Biochem. 86*, 121−130.

Hackney, D. D. (1980) *J. Biol. Chem. 255*, 5320−5328.

Hackney, D. D., & Boyer, P. D. (1978) *Proc. Natl Acad. Sci. U.S.A. 75*, 3133−3137.
Herschlag, D., & Jencks, W. P. (1990) *Biochemistry 29*, 5172−5179.
Kankare, J., Neal, G. S., Salminen, T., Glumoff, T., Cooperman, B., Lahti, R., & Goldman, A. (1994) *Protein Eng. 7*, 823−830.
Kankare, J., Salminen, T., Lahti, R., Cooperman, B., Baykov, A. A., & Goldman, A. (1996a) *Biochemistry 35*, 4670−4677.
Kankare, J., Salminen, T., Lahti, R., Cooperman, B., Baykov, A. A., & Goldman, A. (1996b) *Acta Crystallogr. D* (in press).
Käpylä, J., Hyytia, T., Lahti, R., Goldman, A., Baykov, A. A., & Cooperman, B. S. (1995) *Biochemistry 34*, 792−800.
Knowles, J. R. (1980) *Annu. Rev. Biochem. 49*, 877−919.
Kurganov, B. I. (1982) *Allosteric Enzymes. Kinetic Behavior*, Chapter 4, Wiley, New York.
Lahti, R., Pitkäranta, T., Valve, E., Ilta, I., Kukko-Kalske, E., & Heinonen, J. (1988) *J. Bacteriol. 170*, 5901−5907.
Lahti, R., Pohjanoksa, K., Pitkaranta, T., Heikinheimo, P., Salminen, T., Meyer, P., & Heinonen, J. (1990) *Biochemistry 29*, 5761−5766.
Lahti, R., Salminen, T., Latonen, S., Heikinheimo, P., Pohjanoksa, K., & Heinonen, J. (1991) *Eur. J. Biochem. 198*, 293−297.
Oganessyan, V. Yu., Kurilova, S. A., Vorobjeva, N. N., Nazarova, T. I., Popov, A. N., Lebedev, A. A., Avaeva, S. M., & Harutyunyan, E. H. (1994) *FEBS Lett. 348*, 301−304.
Salminen, T., Käpylä, J., Heikinheimo, P., Kankare, J., Goldman, A., Heinonen, J., Baykov, A. A., Cooperman, B. S., & Lahti, R. (1995) *Biochemistry 34*, 782−791.
Schreier, E. (1980) *FEBS Lett. 109*, 67−70.
Soderling, E., Schneider, G., & Gutterridge, S. (1992) *Eur. J. Biochem. 206*, 729−735.
Springs, B., Welsh, K. M., & Cooperman, B. S. (1981) *Biochemistry 20*, 6384−6391.
Teplyakov, A., Obmolova, G., Wilson, K. S., Ishii, K., Kaji, H., Samejima, T., & Kuranova, I. (1994) *Protein Sci. 3*, 1098−1107.
Terzyan, S. S., Voronova, A. A., Smirnova, E. A., Kuranova, I. P., Nekrasov, Yu. V., Harutyunyan, E. G., Vainstein, B. K., Hohne, W., & Hansen, G. (1984) *Bioorg. Khim. 10*, 1469−1481.
Velichko, I. S., Volk, E. S., Dudarenkov, V. Yu., Magretova, N. N., Chernyak, V. Ya., Goldman, A., Cooperman, B. S., Lahti, R., & Baykov, A. A. (1995) *FEBS Lett. 359*, 20−22.
White, M. F., Fothergill-Gilmore, L. A., Kelly, S. M., & Price, N. C. (1993) *Biochem. J. 291*, 479−483.
Wong, S. C. K., Hall, D. C., & Josse, J. (1970) *J. Biol. Chem. 245*, 4335−4345.

BI952636M